

New Study Of Electrical Conductivity In Ni-Doped Non -Stoichiometric Lithium Tantalite

A. Khalil¹; N. Masaif^{1,2}; A. Jennane^{1,2} and K. Maaider¹

¹ Laboratoire Rayonnement & Matière-Equipe de Recherche Physique de la Matière et Modélisation Faculté des Sciences et Techniques BP 577 Settat, Morocco

² Université Hassan I^{er}, Ecole Nationale des Sciences Appliquées BP 77 Khouribga, Morocco

Abstract: Electrical conductivity in Ni-doped nonstoichiometric lithium tantalite was described by a new theoretical approach. From the experience, we have proposed the new vacancy models which are able to describe substitutional mechanism in Ni-doped lithium tantalite. A combination of phase transition theory and generalised vacancy models allows us to establish a new expression of electrical conductivity which takes into account the defect structure of Ni-doped lithium tantalate. Calculations of the conductivity in Ni-doped nonstoichiometric lithium tantalate reveal good correspondence with experimental results.

I. Introduction

Lithium tantalite (LT) has been the subject of many theoretical and practical investigations due to their properties in electro-optics, electro-acoustics and non-linear optics. This material that shows a ferroelectric behaviour is well known to be narrow-range nonstoichiometric compound. In LiTaO₃, the solid solubility range extends from about 46 to 50.4 mol % of Li₂O at room temperature [1]. The structure of ferroelectric LiTaO₃ belongs to space group R3c and can be considered as a superstructure of the α -Al₂O₃ corundum structure with Li⁺ and Ta⁵⁺ cations along the c-axis [2].

LT compound is ferroelectric at room temperature. It's uniaxial at all temperature, with only a single structural phase transition para-ferroelectric at about 660°C, the precise value depending on the Li/Ta ratio [1] and which is close to a second order one. According to Abrahams and Keve [3], ferroelectricity in this compound is due to the displacements of both the Ta and Li ions within the octahedric sites.

Several studies have reported on the change in electrical conductivity of the Lithium tantalate solid solutions [4], [5], [6], [7], and [8]. By complex impedance spectroscopy

Huanosta et al.⁵ studied the variation of the conductivity as a function of the stoichiometry in Li_{1-5x}Ta_{1+x}O₃ compounds. The LT non-stoichiometric samples present different kind of intrinsic defects to maintain the charge neutrality and therefore can be easily doped by the extrinsic cations, in this way various studies have been performed [6], [9]. Joo et al [9] studied the crystallographic and dielectric properties of LiTaO₃-based non-stoichiometric solid solutions substituted by trivalent ions (Li_{1-x}M³⁺_{x/3})TaO₃, M=Al, Cr, Fe, in and x≤0.20. They showed that

all phases obtained are ferroelectric at room temperature, the Curie temperature T_c decreases when the composition deviates from LiTaO₃. T_c has been related to the size of the M³⁺ cations and to the axial ratio c/a. Torii et al [10] studied the evolution of T_c as a function of doping in (Li_{1-x}M²⁺_{x/2} □_{x/2})TaO₃ with M=Zn, Ni, Mg, Ca. They showed that the change of the Curie temperature was found to be closely related with the c/a ratio of the hexagonal cell. The determination of complex impedances and dielectric permittivities allows one to access to conductivity and dielectric constant and eventually to couple them.

In previous work [11], the successive phase transitions corresponding to the various compositions in LiTaO₃ system have been re-examined. In brief, ceramic specimens of LiTaO₃ with different compositions are studied by the impedance spectroscopy in the 1Hz-1MHz frequency range and the 500-1200 K temperature range. The temperature dependence of the dielectric permittivity of these specimens were measured in order to determine the temperature of the phase transition. So, the ionic conductivity is determined for all compositions from Cole-Cole diagrams. The analysis of the ceramic samples, which are prepared from Li₂O and Ta₂O₅, indicates that there is a modification of the ionic conductivity of LiTaO₃ with Ni content.

While a theory of ferroelectric transition in the crystal LiBO₃ (B=Ta, Nb) has been performed to understand and predict properties of this crystal [12] in this procedure, the solution of the dynamic problem of the crystal planes system exhibits the existence of the "soft mode" at the ferroelectric transition. These recent studies provide a useful understanding of the phase transition dynamic behaviour and the defect structure of LiBO₃.

To find which defect is involved in this phenomenon, we have proposed a theoretical description of the defect structure in LiTaO_3 doped on the basis of a set of vacancy models combined with a ferroelectric phase transition theory.

Finally, we propose quantitative and qualitative defect models in order to interpret some observed phenomena such as change of the Curie temperature and density according to the composition.

In the present paper we study the modification of the electric properties particularly the dc conductivity with Ni doping and those of a slightly non stoichiometric LT (%mol $\text{Li}_2\text{O} = 0.49$) when it is substituted by Ni^{2+} cations up to 20% mol. Ni in relation with the substitution mechanism when the Ni content increases.

II. Experimental Results

The best part of the experimental study has been presented in reference 11 where the experimental procedures are well detailed. In this section, we briefly present the experimental results of solid solutions of the LiTaO_3 doped system. The ceramic specimens of these solid solutions with various compositions were prepared from Li_2O and Ta_2O_5 in stoichiometric quantities.

Ceramics were characterised by X-ray diffraction and the microstructure of these samples were examined using scanning electron microscopy (SEM). The chemical composition of the samples was obtained using inductively coupled plasma-atomic emission spectroscopy (ICP-AES).

The formulae obtained are reported in Table 1. The number of vacancies was calculated by subtraction of the amount of cation sites. The errors in the formulae obtained were estimated to be about 0.8% for Li, 0.1% for Ta and 0.5% for Ni.

For conductivity studies, isothermal measurements were carried out between 600 and 1200 K with temperature steps of 50 or 100 K except in the TC range where steps were reduced to 20K. The instrumentation comprised a Solartron-1260 Impedance Gain Phase Analyzer controlled by a PC computer. The range of measuring frequencies was 1Hz-1MHz for ceramic samples and 1Hz-13 MHz for the single crystal.

The measured conductivities for nonstoichiometric LiNbO_3 with different Ni-doped were shown in figure 1 the form of Arrhenius plots for the temperature range from 830 to 1250 K.

Figure 1 shows the evolution of $\log \sigma$ as a function of $1000/T$ in the 830-1250 K range for Ni-doped LT compositions

Ni%	Formules expérimentales analysées [11]	Modèles proposés
0	$\text{Li}_{0.977}\text{Ta}_{1.005}\text{O}_3$	$[\text{Li}_{0.977}\text{Ta}_{0.005}\text{V}_{0.019}][\text{Ta}]\text{O}_3$
1	$\text{Li}_{0.972}\text{Ta}_{1.002}\text{Ni}_{0.010}\text{O}_3$	$[\text{Li}_{0.972}\text{Ni}_{0.0025}\text{V}_{0.0205}\text{V}_{0.005}][\text{Ta}_{1.0016}\text{Ni}_{0.0075}\text{V}_{-0.0041}\text{V}_{-0.005}]\text{O}_3$
2	$\text{Li}_{0.955}\text{Ta}_{1.001}\text{Ni}_{0.02}\text{O}_3$	$[\text{Li}_{0.955}\text{Ni}_{0.005}\text{V}_{0.03}\text{V}_{0.01}][\text{Ta}_{1.001}\text{Ni}_{0.025}\text{V}_{-0.006}\text{V}_{-0.01}]\text{O}_3$
3	$\text{Li}_{0.942}\text{Ta}_{0.999}\text{Ni}_{0.03}\text{O}_3$	$[\text{Li}_{0.942}\text{Ni}_{0.00375}\text{V}_{-0.0395}\text{V}_{0.09375}][\text{Ta}_{0.9996}\text{Ni}_{0.02625}\text{V}_{0.0079}\text{V}_{-0.03375}]\text{O}_3$
5	$\text{Li}_{0.912}\text{Ta}_{0.998}\text{Ni}_{0.050}\text{O}_3$	$[\text{Li}_{0.912}\text{Ni}_{0.00625}\text{V}_{-0.0745}\text{V}_{0.25625}][\text{Ta}_{0.9976}\text{Ni}_{0.04375}\text{V}_{0.0149}\text{V}_{-0.05625}]\text{O}_3$
8	$\text{Li}_{0.897}\text{Ta}_{0.988}\text{Ni}_{0.08}\text{O}_3$	$[\text{Li}_{0.897}\text{Ni}_{0.01}\text{V}_{-0.157}\text{V}_{0.25}][\text{Ta}_{0.9886}\text{Ni}_{0.07}\text{V}_{0.0314}\text{V}_{-0.09}]\text{O}_3$

Tab.1: Chemical formulae obtained by analysis and proposed formulae, where [.] represents the cations sites and V denotes the vacancies.

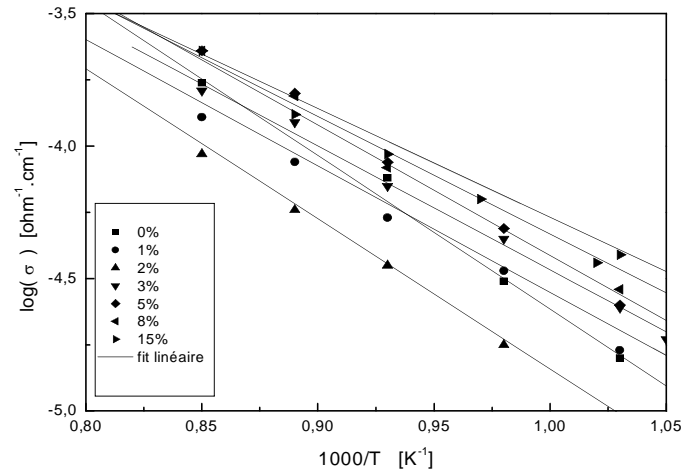


Fig.1: Conductivity Arrhenius plots for different Ni-doped LT

III. Theoretical Approach

In this work, we suppose that ceramic samples of LiTaO_3 are single crystal. Such an assumption is based on the experimental fact that the ferroelectric phase transition occurred in the ceramic samples which are formed by parallel planes along the polar "c" axis. In Figure 2, distances between planes (Li, Ta and O at $T=0$ K) are denoted as follow: $R_{\text{O-O}}(b=2.30\text{\AA})$, $R_{\text{Li-O}}(R_{20}=0.601\text{\AA})$, $R_{\text{Ta-O}}(R_{10}=0.954\text{\AA})$, $R_{\text{Li-Ta}}(R_{12}=b - R_{10} - R_{20})$ [13].

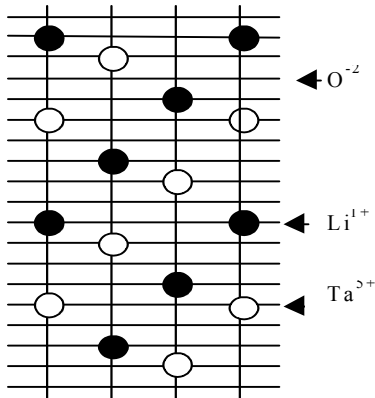


Fig. 2: Different planes in an elementary cell of crystal LiTaO_3 .

Safaryan's new approach on ferroelectric transition in the crystal LiNbO_3 is newly tested in the LiTaO_3 compound in order to discuss the main role of the nonstoichiometric compositions. We avoid the detail of the theory of ferroelectric transition in the crystal LiTaO_3 which is similar to that of reference [12] and only report the useful expressions in the appendix. At

0°K, the soft mode frequency, ω^2 , is proportional to the Curie temperature. Substituting ω^2 to obtain the following relation that allows calculating the Curie temperature [14]:

$$\frac{T_c^*}{T_c} = \frac{M_1^* + M_2^* + M_0^*}{M_1 + M_2 + M_0} \left(\frac{M_1 M_2 M_0}{M_1^* M_2^* M_0^*} \right) \left(\frac{P_1^*}{P_1} \right) \left(\frac{P_2}{P_2^*} \right) \quad (1)$$

With

$$P_1^* = 3q_0^* R_{12}^2 - q_1^* R_{20}^2 - q_2^* R_{10}^2$$

And

$$P_2^* = \frac{(R_{20} R_{21})^2}{q_2^*} \left(\frac{1}{M_1} + \frac{1}{M_0} \right) + \frac{(R_{10} R_{21})^2}{q_1^*} \times \left(\frac{1}{M_2} + \frac{1}{M_0} \right) - \frac{(R_{10} R_{20})^2}{3q_0^*} \left(\frac{1}{M_1} + \frac{1}{M_2} \right)$$

The elements X represents the exact stoichiometric composition and X^* is the nonstoichiometric doped compositions.

The Electrical conductivity can be described by the law of Arrhenius

$$\sigma = \sigma_0 \exp\left(-\frac{\Delta E}{k_B T}\right) \quad (2)$$

Where σ_0 is the pre-exponential factor, ΔE the activation energy, k_B the Boltzmann constant and T is the temperature (K).

We introduce the conductivity, σ^* , to explain the role of defect structure in nonstoichiometric doped lithium tantalate compound such that.

$$\sigma^* = \sigma_0^* \exp\left(-\frac{\Delta E^*}{k_B T^*}\right) \quad (3)$$

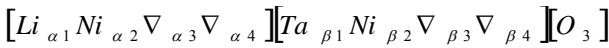
With X^* related to nonstoichiometric doped compositions.

Although the expression of the T^* is determinate at Curie temperature point, this relation seems again correct to calculate the conductivity about T^* . Taking into account of the experimental results[11], we have proposed two possible models for explaining

- Model (a) : $[Li_{1-5x-3y}Ni_{1y}\nabla_{5x}\nabla_{2y}][Ta_{1+(x-y)}Ni_{3y}\nabla_{-x}\nabla_{-2y}][O_3]$ (Ni<3%)
- Model (b) : $[Li_{1+5x-13y}Ni_{\frac{1}{2}y}\nabla_{-5x}\nabla_{\frac{25}{2}y}][Ta_{1-(x-y)}Ni_{\frac{7}{2}y}\nabla_x\nabla_{-\frac{9}{2}y}][O_3]$ (Ni ≥ 3%)

Where ∇ represent the vacancy.

We represent these models, described previously, in the following condensed form,



And $K^* = g K$

With $K=M$, q and $g=\alpha, \beta$. Here α and β allow the two models to be identified as follows:

- i) Model (a) corresponds to $\alpha_1=1-5x-3y$, $\alpha_2=1y$, $\beta_1=1+x-y$, $\beta_3=3y$; and $K_2^* = \alpha_1 K_2 + \alpha_2 K_3$, $K_1^* = \beta_1 K_1 + \beta_2 K_3$ and $K_0^* = K_0$.

the solid-solution mechanism of LiNbO3 doped. The first will be valid for concentrations% Ni <3% and the second for the concentration% Ni ≥ 3%

- ii) Model (b) corresponds to $\alpha_1=1+5x-13y$, $\alpha_2=1/2y$, $\beta_1=1-x+y$, $\beta_2=7/2y$; and $K_2^* = \alpha_1 K_2 + \alpha_2 K_3$, $K_1^* = \beta_1 K_1 + \beta_2 K_3$ and $K_0^* = K_0$.

In this representation $\alpha=\beta=0$ signified that ions and vacancies are absent in these nonstoichiometric models. In order to provide an adequate description of the structure LTaO3 doped with Ni we have analytically performed the calculations of the Curie temperature as function of the composition x and y that we illustrate in Table 3. Estimate values of for LiTaO3 have been obtained using the following values of charges and masses of ions $q_0=2$, $q_1=5$, $q_2=1$, $q_3=2$, $M_0=48$, $M_1=180.95$, $M_2=6.94$, $M_3=58$.

The conductivities for these vacancy models could, therefore, be calculated according to equation (3) taking into account the values of the σ_0 and ΔE for each composition x and y .

	Model (a)	Model (b)
T_c^*	$T_c^* = \frac{(1+1,089x+0,233y)}{(1-4,925x+2,129y)} T_c$	$T_c^* = \frac{(1-1,089x+2,507y)}{(1+4,925x-10,406y)} T_c$

Tab.3: The Curie temperature T^* as a function of the nonstoichiometric composition x and rate doping y . (b) and (c) represent the vacancy mod

IV. Results

In principle, one could test these models by comparing the experimental results with the calculated values of the conductivities from this theoretical approach. To explain the effect of doping on the conductivity, we have applied the results of the procedure to a discussion of the interpretation of the experimental data. To calculate the Curie temperatures suggested in Table 3 we have needed to know the Curie temperature of the exact stoichiometry compositions. So, we have used the following estimations of the Curie temperatures in the stoichiometry lithium tantalate 938 K [15], 917 K [11] and 948 K [16]. The average values of these estimations are =934 K.

By a linear fit of the experimental values and the calculation of the slope of the $\log \sigma$ curve in the form of Arrhenius plot (figure 1) we obtained σ_0 and ΔE for different Ni-doped LT. The calculated and experimental values of σ^* for various nonstoichiometric doped compositions are illustrated in Figures 1, 2, 3, 4, 5 and 6. For each Ni content, we note that the conductivity increases with increasing temperature. Comparing the measured conductivity for nonstoichiometric LiTaO3 with the two vacancy models (model (a) and model (b)), the results demonstrate clearly that the calculated values are in a good agreement with the data obtained by the experimental study.

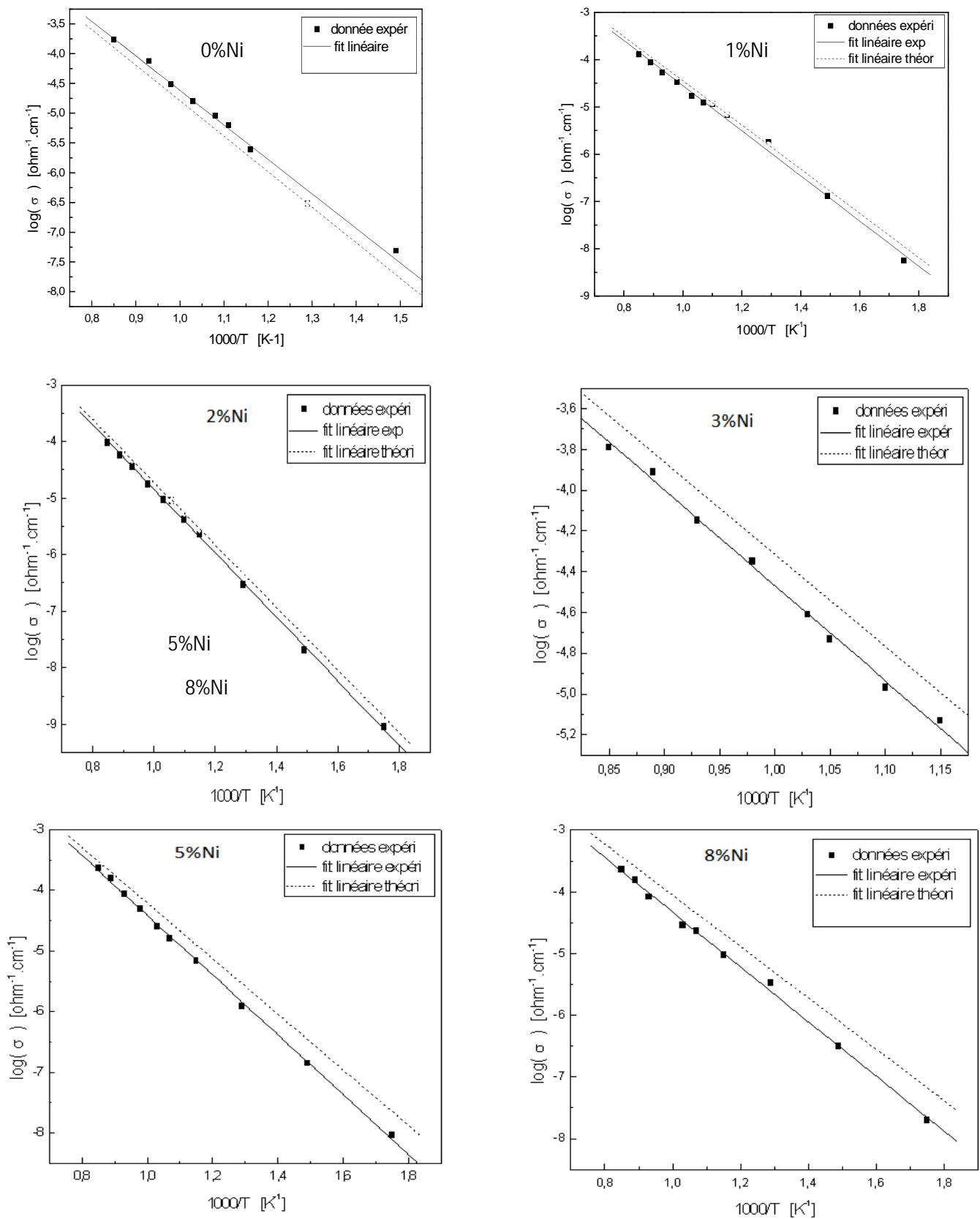


Fig.3: Logarithmical conductivity of LiTaO₃ solid solutions as a function of the reciprocal temperature with the Ni content, for 0, 1, 2, 3, 5 and 8%Ni. The full triangles are the experimental data and the solid lines represent the linear fits to the data.

In order to examine the influence of Ni doping on dc conductivity of our samples we have represented at fixed temperatures its evolution with Ni content in Fig.4.

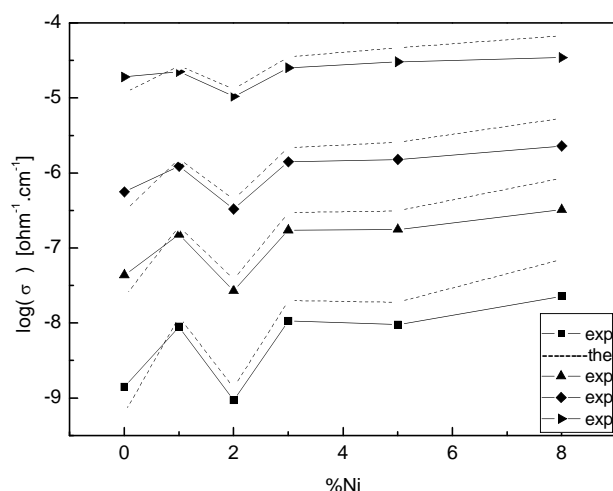


Fig. 4: Evolution of dc conductivity with Ni content at fixed temperature

V. Discussion

The influence doping on Conductivity is quantitatively analyzed on the basis of a simplified structural description of lithium tantalate.

The results illustrated in Figs. 3 illustrated that:

- The calculated values are in a good agreement with the data obtained by the experimental study.
- Application of the theory based on the structure simplified, combined with theoretical models vacancies (α) and (β), in ionic conductivity passed very close to the experimental data.
- All straight lines for doped samples are practically parallel, with a slope slightly different from that of the pure sample.
- The conductivity increases with the Ni content except for the 2% Ni-doped compound for which the conductivity is smaller than that observed for the 0% and 1% Ni-doped compounds. The anomaly observed for $y=2\%Ni$ can be related to the modification of the mechanism of substitution of nickel cations in the lattice when the NiO content is greater than about 2.5%. Taking into account the model (a), the prepared pure LT should have the chemical formula $[Li_{0.977}Ta_{0.005}V_{0.019}][Ta]O_3$. When Ni cations are inserted in the lattice, it is thus probable that they are preferentially located on the lithium sites and replace all the tantalum atoms. From formulae given in Table 1, it is seen that this is obtained for a Ni content comprised between 2 and 3%. This deranges the structure and complicates the motion of Li ions; consequently we obtain the decrease of ionic

conductivity. For higher Ni contents (model (b)), For example, for $y = 5\%Ni$. Ni ions occupy simultaneously the vacants Li and Ta ions sites, dc conductivity increases with Ni content. Indeed, there are no Ta ions in Li-sites, the number of vacancies increases with the introduction of Ni, also Li and Ni ions have approximately the same ionic radius ($R_{Li} \approx R_{Ni} = 0.69 \text{ \AA}$); the motion of both Li and Ni ions contributes simultaneously to conduction, and increases the dc conductivity.

Fig.4 shows plots of the conductivity as function of contenu Ni for various fixed temperatures. In this Figure, The conductivity increases with the Ni content except for the 2% Ni-doped compound. We have therefore used this theory for a consistent study of vacancy defects in doped LN using the available vacancy models. In our compounds, that is to say non-stoichiometric doped LN.

VI. Conclusion

We have presented the conductivity as a function of the temperature and of the Ni content in the Ni-doped series. In this simple system, the theory of ferroelectric phase transition gives a good quantitative description of the experimental results.

Application of the theory based on the structure simplified, combined with theoretical models vacancies (a) and (b), in ionic conductivity is a fruitful way to describe the structure of $LiTaO_3$ ceramics doped with nickel

The vacancy model (a) and (b) is quantitatively and qualitatively imposed as the best model to interpret extrinsic defect structure in lithium tantalate.

VII. References

- [1] M. Paul, M. Tabuchi, A. R. West, Chem. Mater., **9** (1997) 3206.
- [2] S. C. Abrahams, L. J. Bernstein, Phys. Chem. Solids, **28** (1967) 1685.
- [3]-S.C. Abrahams and E. T. Keve ; ferroelectrics, **2**, 129, 1971
- [4]-R. L. Barns and J. R. Carruthers, J.appl Crystallog **V3**, P395, 1970.
- [5]-A. Huanosta and A. R. West, J. apply phys **61** (12), 1987.
- [6]-D. C. Sinclair and A. R. West Physical review B, **V39**, N18, 1989
- [7]-Tomono I., S. Matsumura, Phys. Rev, **B38** (1988)606.
- [8]-D. Ming, J.M.Reau, J. Ravez, J. Gitae, and P. Hagenmuller, J. solid state chem., 1995, **116**, 185
- [9]-G. Joo, J. Ravez, P. Hagenmuller, Revue de chimie minerale, **t22**, p18, 1985.
- [10]-Y. Torii, T. Sekiya and T. Yamamoto, Kei

- Koyabachi, and Yoshihiro Abe, Mat. Res. Bull; **V18**, pp1569-1574,1983.
- [11]- F. Bennani, E. Husson, J of European Ceramic Society, 21 (2001) 847.
- [12]- F. P. Safaryan., Physics Letters A, 191, 255 (1999).
- [13]- M. E. Lines, A. M. Glass, Principles and application of ferroelectrics and related materials. Clarendon Press, Oxford (1977).
- [14]- N. Masaif, S. Elhamd, S. Jebbari, A. Jennane and F. Bennani
- [15]- H. D. Megaw., Acta. Cryst., 7, 187 (1954).
- [16]- R. L. Barns and J. R. Carruthers., J. Appl. Crystallog.,3,395(1970).